Power Electronics and Drives
Volume 7(42), 2022 DOI: 10.2478/pead-2022-0010

Automated UAV to Survey and Monitor Ionising Radiation Levels in a Closed Environment

Research paper

Anand R.[1]*, Harshith Kumar M. B.[2], Anirudh Raghavan[2], Roopak Maddara[2], Prajna Anand[3]

[1]*Otis Elevator Company, Research and Development, Bangalore, India*
[2]*Department of Electronics and Communication Engineering, PES University, Bangalore, India*
[3]*School of Computer Science Engineering, RV University, Bangalore, India*

Received: April 25, 2022; Accepted: July 09, 2022

Abstract: Since tragedies caused by nuclear disasters are always a concern, it is essential that nuclear power plants be monitored on a regular basis for any irregularities in ionising radiation levels. Irrespective of leakage proof measures being deployed in the plant, ensuring the safety of these measures is necessary. Given this scenario, the present study proposes the usage of unmanned aerial vehicles (UAVs) to ensure that radiation levels in nuclear plants remain within safe limits. The UAV deployed will map the entire environment following a unique path planning algorithm and monitor the environment with an onboard radiation sensor. If any irregularities are detected, the positional coordinates are flagged, and the A* algorithm is implemented to generate the shortest path between the starting point, and the flagged coordinates, which are considered as the destination coordinates. The UAV is made to traverse the shortest path together with maintaining stability of the system while traversing.

Keywords: *unmanned aerial vehicle • indoor SLAM • sensor data • disaster management robots • path planning • obstacle avoidance*

1. Introduction

In recent times, aerial robotic systems have been in use during calamities and in rescue operations. Unmanned aerial vehicles (UAVs) provide the facility of gaining at least electronic (surveillance) access to environments where human access is restricted, or as in some cases, difficult.

Considering a situation of a nuclear power plant, the indoor environment, being prone to radiation leakages, is proven to be fatal. Continuous monitoring of the environment for radiation levels provides a bigger picture of the calamity.

Recognising the highly affected regions in the indoor environment of the power plant is of immense importance to avoid and contain radiation at early stages. The usage of UAV proves to be better than manual intervention in such critical environments. The onboard sensor (Čerba et al., 2020), providing the data about the radiation intensities, is vital for recognition of the affected regions.

With these procedures in hand, the UAV is expected to map the indoor environment, collect the sensor data at various locations, and pinpoint critical points in the environment. In the end, it would generate a shortest path from the entrance of the environment to the epicentre passing through the flagged critical points.

The prioritised affected areas can be noted by the sensor data. The onboard sensor data provide the reading at all the coordinates. When the sensor readings are at their highest peak, it can be confirmed that the epicentre is at the corresponding coordinates.

The article is structured as follows: Section 2 is dedicated to discussing relevant studies in the literature, Section 3 discusses the state space model of the UAV, Section 4 proposes the methodologies, and Section 5 covers the experimental results arrived at. Finally, Section 6 concludes the paper together with mentioning the future scope.

* *Email: anandprajna@gmail.com*

2. Relevant Works

In recent years, significant research has been conducted in terms of enhancing the technology involved in the surveillance and mapping of environments. Specifically, for radiation detection, multiple approaches have been proposed and implemented. Some of them are discussed here.

Aleotti et al. (2015) discuss UAVs that are deployed to detect the presence of a few of the radioactive elements using spectroscopic detectors, while Rudolph et al. (2020) propose a comparable data evaluation method for a radio-nuclear sensor when used on an UAV.

Usage of UAVs to specifically detect gamma radiation using an onboard sensor is an ongoing subject of research, with some studies, e.g. Hartman et al. (2015) and Pani et al. (2019), already describing this method's implementation. While Duck et al. (2017) propose a system to detect gas as well as radiation using UAVs as well as a handheld module, Cai et al. (2016) have developed a prototype radiation detection and mapping UAV system to safely identify irradiated areas in the event of a nuclear emergency.

With respect to the manoeuvring of UAVs in confined as well as open air environments (Bhattacharyya and Baum, 2018; Krátký et al., 2021; Morita et al., 2018), the implemented algorithms provide evidence for the successful detection of radiation in a variety of environments.

In nuclear power plants, it is essential to monitor the incoming and outgoing manual workforce as well as vehicles for possible radiation carriages. This was implemented by Wan Seo et al. (2021).

Additionally, while detection of radiation levels is one aspect, communicating the UAV sensor data back to the ground station (Micconi et al., 2016; Reyes Munoz et al., 2015) is also essential so that the manual procedures can be initiated accordingly to prevent any escalation of calamity.

3. System Description

Whenever a robotic system is taken into consideration, it is essential to ascertain the various forces that act on it, and thus arrive at the means of providing for the counter forces that the robot would need to exert, in order to nullify the external forces. In this work, since we are considering an UAV, the system has 6 degrees of freedom (DOFs); but for this particular work, we consider the linear motion in *x*, *y*, and *z* directions (as shown in Figure 1).

The system is assigned with a state space model that mentions the input force and the resultant output of the system in a mathematical form.

$$\dot{x}(t) = Ax(t) + Bu(t) \tag{1}$$

$$y(t) = Cx(t) + Du(t) \tag{2}$$

In the above equations, $y(t)$ is the output vector and $u(t)$ is considered the input/control vector.

In this work, the above equations are assigned the following matrices, considering the weight of the robotic system to be 1.2 kg, and other forces such as gravity and air resistance.

Further, we consider only the x and y direction motion of the UAV as the UAV maintains a stable altitude while it is being traversed across the environment.

Since the *x* and *y* direction motions are countered by the air resistance in itself, in case of indoor environment, the obstacle reverts the force exerted on it by the motors of the UAV. The state space model is designed considering the additional frictional resistance as an opposing force for the robot.

$$\mathrm{A} = \begin{matrix} 0 & 1.2 \\ 0.833 & 0 \end{matrix} \tag{3}$$

$$\mathrm{B} = \begin{matrix} 0 \\ 0.833 \end{matrix} \tag{4}$$

$$\mathrm{C} = 1 \quad 0 \tag{5}$$

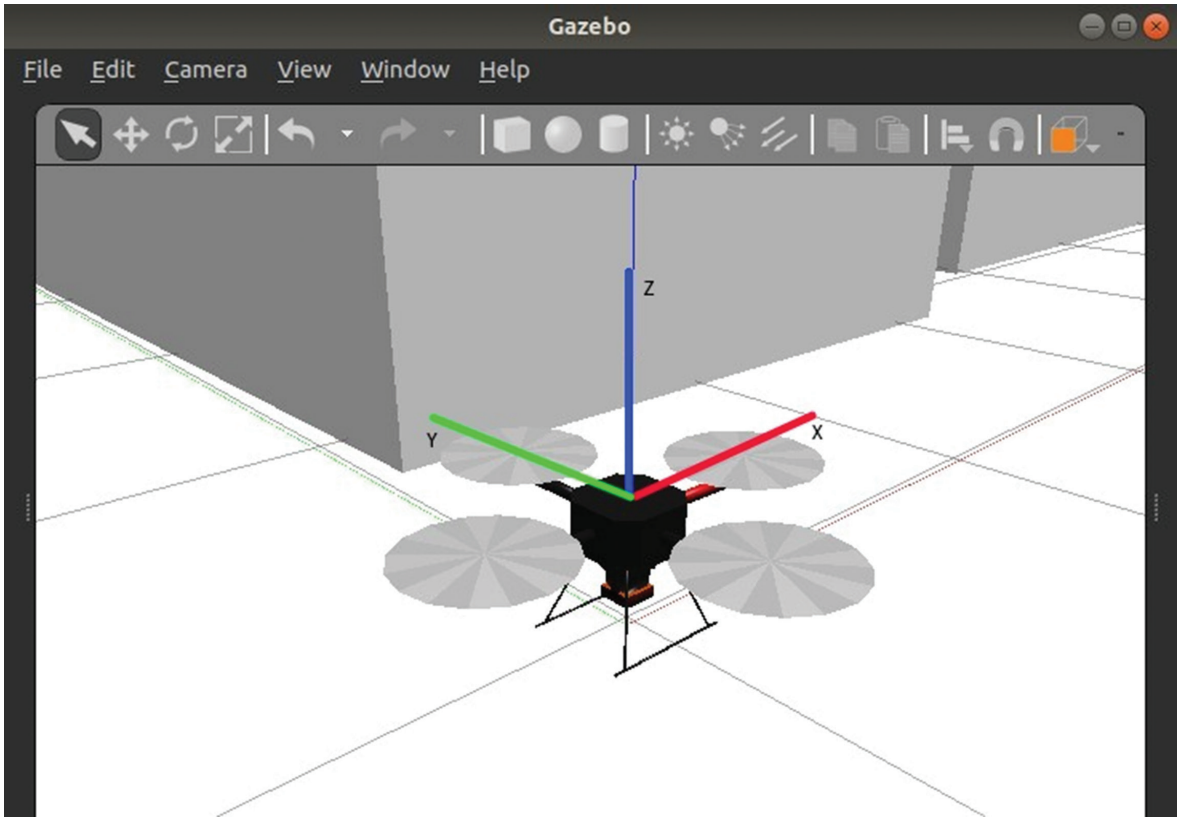

Fig. 1. *x*, *y*, and *z* directions of the UAV. UAV, unmanned aerial vehicle.

Taking the above matrices into consideration, the state transfer function arrived at is the following:

$$G(s)=\frac{1.2}{s^2+1} \tag{6}$$

The formulation is arrived at using the following expression:

$$G(s)=C([sI-A])^{-1}B \tag{7}$$

where *I* is the identity matrix.

4. Methodology

The unique aspect lies in the methodology, or the approach followed to achieve the end result. The UAV used in the indoor environment of a nuclear power plant to localise the leakage and in mapping the whole environment to detect the radiation concentration provides a bigger picture into the intensity of the leakage. Further, since the operations are undertaken in a confined space, the precision in positional navigation plays a major role.

4.1. Environment development and mapping

The indoor environment represents a closed location with narrow pathways. The UAVs are expected to travel across the environment, avoiding any possible collisions with the walls or dynamic obstacles. The indoor environment is built in Gazebo Simulator, which is a robot operating system (ROS). The indoor environment is unknown to the UAV system. Thus, both the pathways and the positions of the obstacle need to be mapped.

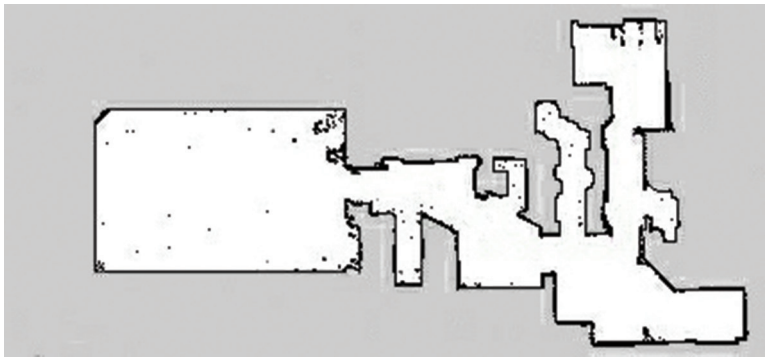

Fig. 2. An image of the map considered to build an indoor environment.

The Gazebo environment takes in an image of a map (as shown in Figure 2) into consideration. Using the unified robot description format file of the environment, a launch file is created. The launch file varies the size, position, and orientation of the image that specifies the indoor environment.

The UAV is iterated for the first time across the environment. The UAV traverses across the environment based on the sensor data provided by the onboard Lidar or the 'LaserScan' Rostopic available onboard. Based on the readings, the presence of pathway and obstacles (both static and dynamic) is detected.

4.2. Path planning

The path planning algorithms in this work rely on the inertial measurement unit (IMU) data for tracking the UAV's position in the environment. This allows the system to localise all the obstacles and essential positional coordinates. Further, this results in considering the take-off position as the origin. Since the UAV system takes off twice, it is to be noted that the system needs to take off from the same position and orientation for the second time.

4.2.1. First iteration – Instinctive motion of the UAV

As the UAV is supposed to map the unknown environment, the instinctive path planning algorithm provides a better decision-making opportunity for the UAV. Here, a variable named 'target' is defined, where the 'target' changes its value according to the path to be traversed and based on environment in which the UAV manoeuvres through.

In the environment, when the UAV doesn't face any junctions or obstacles in front, the target increments its value in the forward direction. And similarly, wherever the obstacles are detected, the target coordinates vary opposite to the direction of the obstacle.

Algorithm 1: Pseudocode describing the instinctive path planning.

```
Data:    Output from LaserScan Rostopic
Result:  Decision by UAV on Path to be taken

while (extended obstacle detected in the front of the UAV):
# a junction is arrived where the path in front is unavailable
if (obstacle detected at right is farther from that detected on the left):
        if (path is unexplored):
          target = target increment towards the right
          rotate rightwards
        else:
          target = target increment towards the left
          rotate leftwards
else if (obstacle detected at left is farther from that detected on the right):
```

```
            if (path is unexplored):
        target = target increment towards the left
                rotate leftwards
            else:
              target = target increment towards the right
              rotate rightwards
        else:
           target = target increment towards front
    end
  end
```

On the other hand, when at junctions through which the UAV has already traversed, the target coordinates are varied in such a way that the same path is not traversed multiple times. At every variation in the target coordinates, the coordinates are recorded. Through this methodology, it is ensured that all the corners and junctions of the environment are iterated and mapped.

Once the whole of the environment is mapped, the UAV returns to its initial position, i.e. to the origin. The UAV traverses every set of 'target' coordinates smoothly using the proportionality, integral, and derivative (PID) controller, where the error value for the controller turns out to be the distance between the target coordinates and the present UAV positional coordinates.

4.2.2. Generating the shortest path across the environment

Once the map is generated after the mapping during the first iteration, the corresponding sensor data are also taken into consideration along with the coordinates to pin-point the coordinates of the epicentre of the leakage. Once the target coordinates are finalised, the A* algorithm is programmed to generate the shortest path considering the coordinates and sizes of the obstacles as specified by the map generated.

The A* algorithm generates the shortest path that the UAV traverses to arrive at the epicentre of the leakage from the point of lift-off.

4.3. PID controller

Since the path generated by the A* algorithm requires the UAV to manoeuvre from one coordinate to another, the UAV needs a controller to control its speed so that the coordinates are traversed without any overshoot and delay. This is taken care of by the PID controller. The PID controller is provided with three constants Kp, Ki, and Kd, manipulating each of the individual controllers.

The PID controller works on a feedback system. Here the error function is the difference between the target and present positions of the UAV.

4.4. Obstacle avoidance

The obstacle avoidance plays a vital role in the indoor environment scenario as the walls stay close to the UAV system. The sensor data always reads the presence of obstacles. The walls in the indoor environment act as a static and continuous obstacle. Initially, when the mapping procedure is in process, the obstacle avoidance helps the drone in making decisions at the diversions.

Along with this, the dynamic obstacles can also be tackled. As the dynamic obstacle approaches the UAV, the nearer the obstacle is, the swifter the UAV manoeuvres against that direction in order to avoid collision.

In this process, the PID controller is used again. The only change is that the error function in the case of the obstacle avoidance algorithm will be the inverse of the distance between the obstacle and the UAV system, thus making it reactive when a dynamic obstacle is encountered.

4.5. Sensor data of radiation sensors

The onboard ionising radiation sensor (as shown in Figure 3) will play a vital role in recognising the radiation-affected regions in the indoor environment. The sensor used in this work is a radiation sensor board with the SBM-20 Geiger Tube.

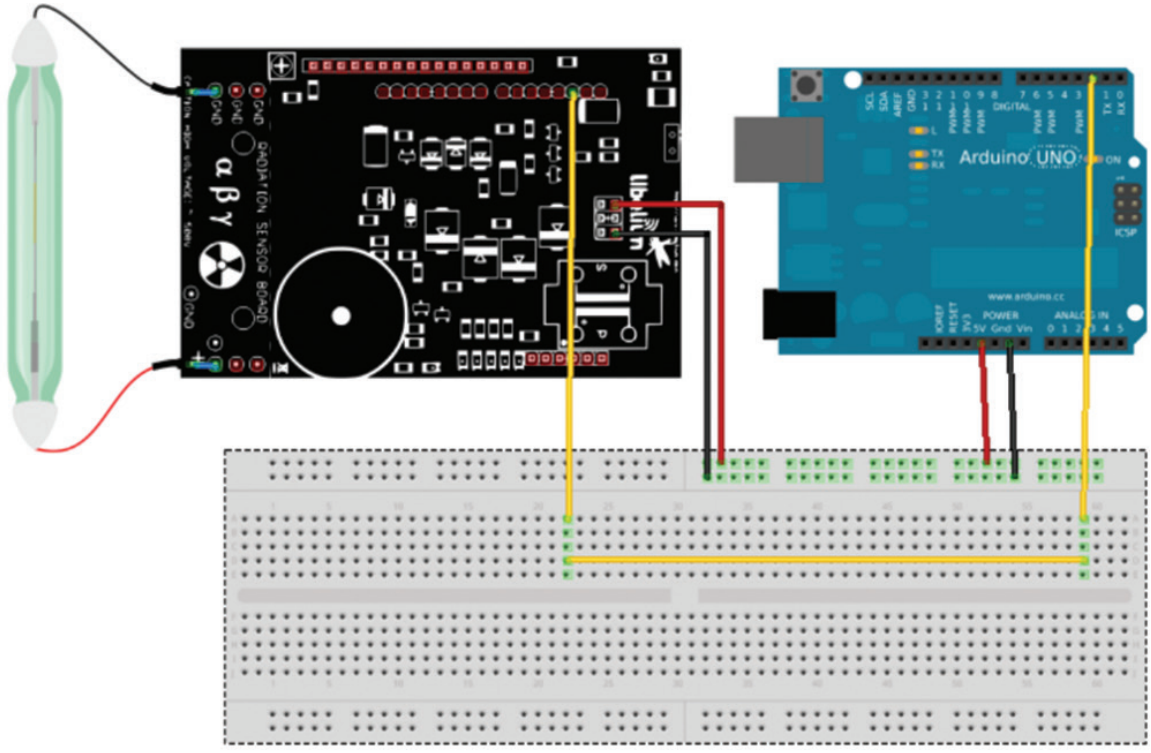

Fig. 3. The circuit diagram of onboard radiation sensor with Arduino.

The data logging takes place in such a way that the .csv file consists of UAV coordinates and their corresponding sensor readings. Thus, the highest surge in sensor data represents the region affected by harmful radiations.

4.6. Kalman filter

The Kalman filter provides the most probable yet accurate estimation of the position of the UAV based on the IMU sensor data. This work uses IMU data rather than a GPS module, since the environment is indoor, and thus GPS readings may show errors. Thus, using a Kalman filter proves mandatory in ensuring that the position estimation of the UAV is carried out accurately.

The Kalman filter works in three steps. The first is to estimate the future position of the UAV in the immediately succeeding time interval. The second is to measure the actual distance travelled by the UAV. The final step is to update the estimation process. The prediction and updating algorithm follow the following equations:

Prediction:

$$X'_k = A_{k-1}X_{k-1} + B_kU_k \tag{8}$$

$$P'_k = A_{k-1}P_{k-1}A^T{}_{k-1} + Q_{k-1} \tag{9}$$

Updating:

$$V_k = Y_k - H_kX'_k \tag{10}$$

$$S_k = H_kP'_k\,H^T{}_k + R_k \tag{11}$$

$$K_k = P'_k\,H^T{}_k + S^{-1}{}_k \tag{12}$$

$$X_k = X'_k + K_kV_k \tag{13}$$

$$P_k = P'_k - K_kS_kK^T{}_k \tag{14}$$

where X' indicates the predicted mean value before processing the measured space; P' the predicted covariance value before processing the measured space; X the estimated mean value after processing the measured space; P the predicted covariance value after processing the measured space; V the measurement residual on a particular time step; Y the mean of the measurement at a particular time step; S the measurement prediction covariance; and finally, K represents the filter gain.

5. Experimental Results

Pursuant to implementing the above algorithms and methodologies using the UAV model, the following results have been arrived at.

According to the theoretical concepts, it is necessary to achieve stability of the system using a PID controller. For the transfer function derived for the UAV, a unity feedback system is formulated. The stability was achieved within the desirable minimum time for following constant values constituting the PID controller.

$$Kp = 10,\ Kd = 12.5,\ Ki = 1.2$$

Figure 4 represents the stability achieved when a step signal was used as an input for the system. And likewise, Figure 5 represents the stability achieved when a ramp response was used as an input for the system.

With the theoretical stability achieved, the UAV was tested for the instinctive movement in the indoor environment to detect the epicentre of the gas mishap. The gradual mapping results were observed (as shown in Figure 6), where the UAV recognised the obstacles around it and localised them.

In the end, the whole of the indoor environment was successfully mapped, and respective radiation sensor data were also logged, as shown in Figure 7, to localise the regions affected by radiation. The sensor data are divided by 10 to get the exact value of radiation concentration in terms of millirems. It is detected that 10 mrem/day is the higher end of safety threshold of radiation. Any readings higher than 10 mrem are considered to be harmful for humans.

With the map being generated, using the A* algorithm, the shortest path was generated from the point where the UAV took off to the target coordinates. The shortest path ensures that all the static obstacles detected are avoided and thus helps in smooth manoeuvring of the UAV to the target coordinates.

The generated coordinates were plotted using matlab, which provided the line path. The coordinates are determined as (0, 0) for the take-off coordinates and (33, –1) for the target coordinates.

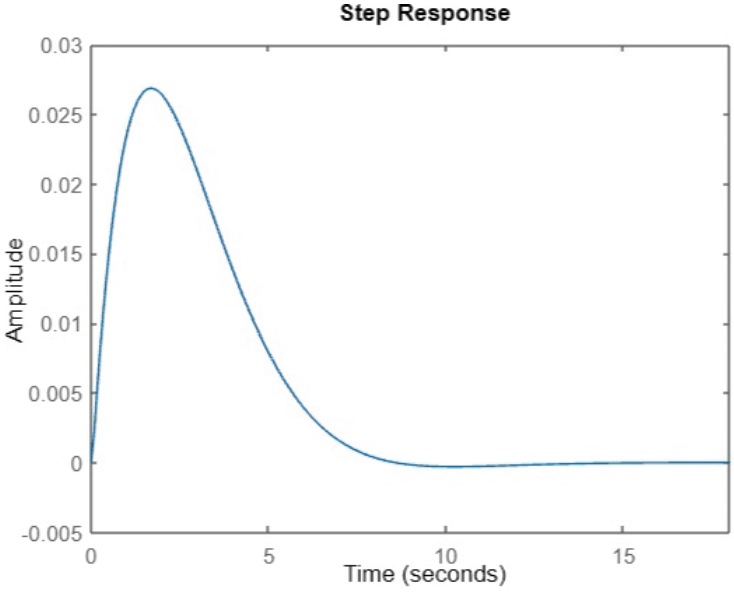

(Amplitude = error between the target and present positions of the UAV)

Fig. 4. Output of the unity feedback system of UAV with step signal as input. UAV, unmanned aerial vehicle.

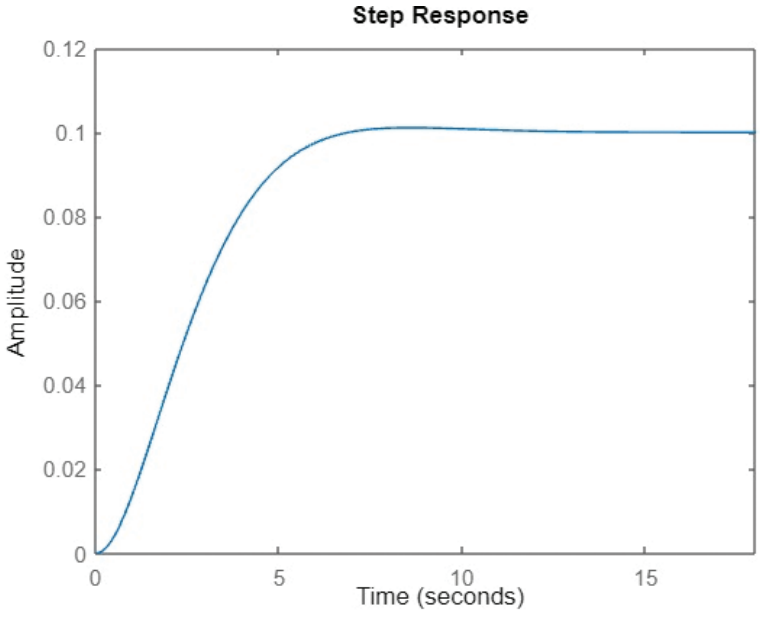

(Amplitude = present position of the UAV in a single direction)

Fig. 5. Output of the unity feedback system of UAV with ramp signal as input. UAV, unmanned aerial vehicle.

Fig. 6. Stages of mapping of the environment.

Figure 8 provides a visualisation of the path when plotted using the line graph. Additionally, Figure 9 provides the results where the coordinates are generated when the A* algorithm is implemented on the collected data and maps.

As the coordinates are generated, the UAV is now successfully navigated over each of the coordinates and arrives at the destination coordinates. The traversal of the UAV in the environment is as shown in Figure 10.

	A	B	C	D	E
1	Timestamp	Sensor Data	Coordinates		
2	02:02:22:17:693	Initialising MQ4... Sensor starting up	(0,0,0)		
3	02:02:22:17:902	Reading Data	(0,0,0.5)		
4	02:02:22:18:251	62	(0,0,1)		
5	02:02:22:18:479	62	(0,0,2)		
6	02:02:22:18:711	62	(0.4,0,2)		
7	02:02:22:19:027	63	(1,0,2)		
8	02:02:22:19:310	63	(1.5,0,2)		
9	02:02:22:19:451	63	(1.6,0,2)		
10	02:02:22:20:004	63	(2.2,0,2)		
11	02:02:22:20:298	63	(3,0,2)		
12	02:02:22:20:512	63	(3.5,0,2)		
13	02:02:22:20:693	63	(4.1,0,2)		
14	02:02:22:20:994	75	(6,0,2)		
15	02:02:22:22:001	82	(6.7,0,2)		
16	02:02:22:22:215	82	(7.3,0,2)		
17	02:02:22:22:661	82	(8,0,2)		
18	02:02:22:23:004	83	(8.8,0,2)		
19	02:02:22:23:215	82	(9.3,0,2)		
20	02:02:22:23:516	83	(9.4,0,2)		
21	02:02:22:24:007	82	(9.6,0,2)		
22	02:02:22:22:008	82	(0,0,2)		

Sheet1

Fig. 7. Logged data of radiation sensor module with corresponding positional coordinates.

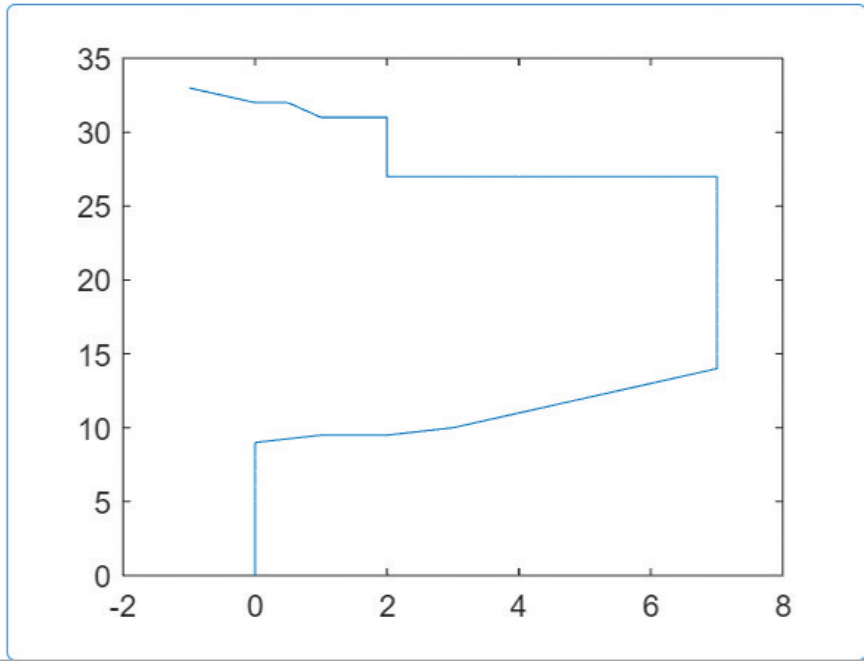

Fig. 8. Line plot of shortest path generated by A* algorithm.

While the mapping and path planning algorithms successfully automate the UAV to its goal, the position estimation by the Kalman filter ensures accurate estimation for furthering the smoothening of the UAV's motion.

```
:~/Desktop$ python p.py
[[0, 0], [1, 0], [2, 0], [3, 0], [4, 0], [5, 0], [6, 0], [7, 0], [8, 0], [9, 0]
, [9.5, 1], [9.5, 2], [10, 3], [11, 4], [12, 5], [13, 6], [14, 7], [15, 7], [16
, 7], [17, 7], [18, 7], [19, 7], [20, 7], [21, 7], [22, 7], [23, 7], [24, 7], [
25, 7], [26, 7], [27, 7], [27, 6], [27, 5], [27, 4], [27, 3], [27, 2], [28, 2],
 [29, 2], [30, 2], [31, 2], [31, 1], [32, 0.5], [32, 0], [33, -1], [33, -1]]
```

Fig. 9. Coordinates generated by A* algorithm.

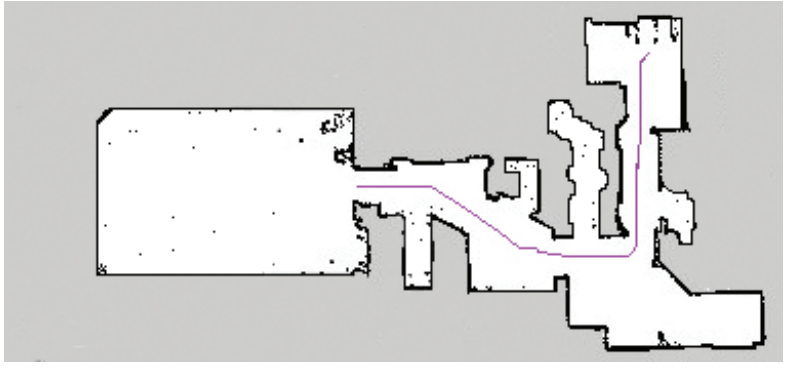

Fig. 10. Traversal track of UAV based on path generated by A* algorithm. UAV, unmanned aerial vehicles.

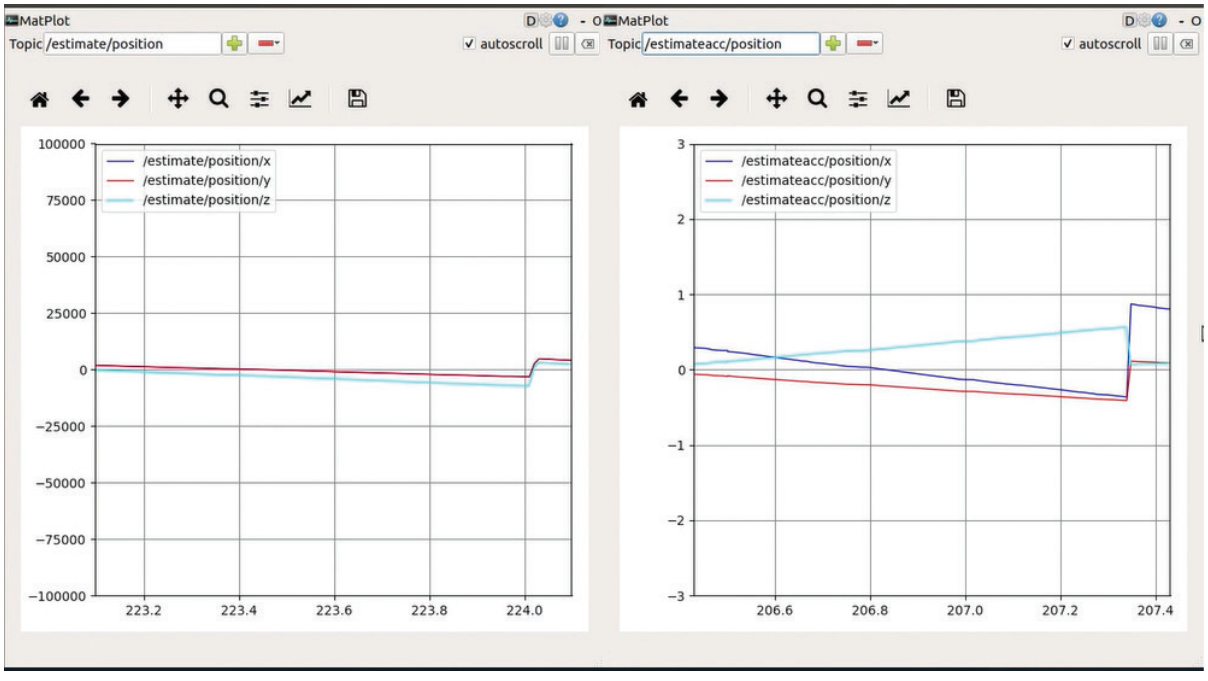

Fig. 11. Error comparison of position estimation without (left window) and with (right window) Kalman filter.

From Figure 11 it is observed that the error estimation oscillates between enormous values when the Kalman filter is not in use. On the other hand, it is observed that with the use of Kalman filter, the same error is drastically attenuated, ensuring higher accuracy of position estimation.

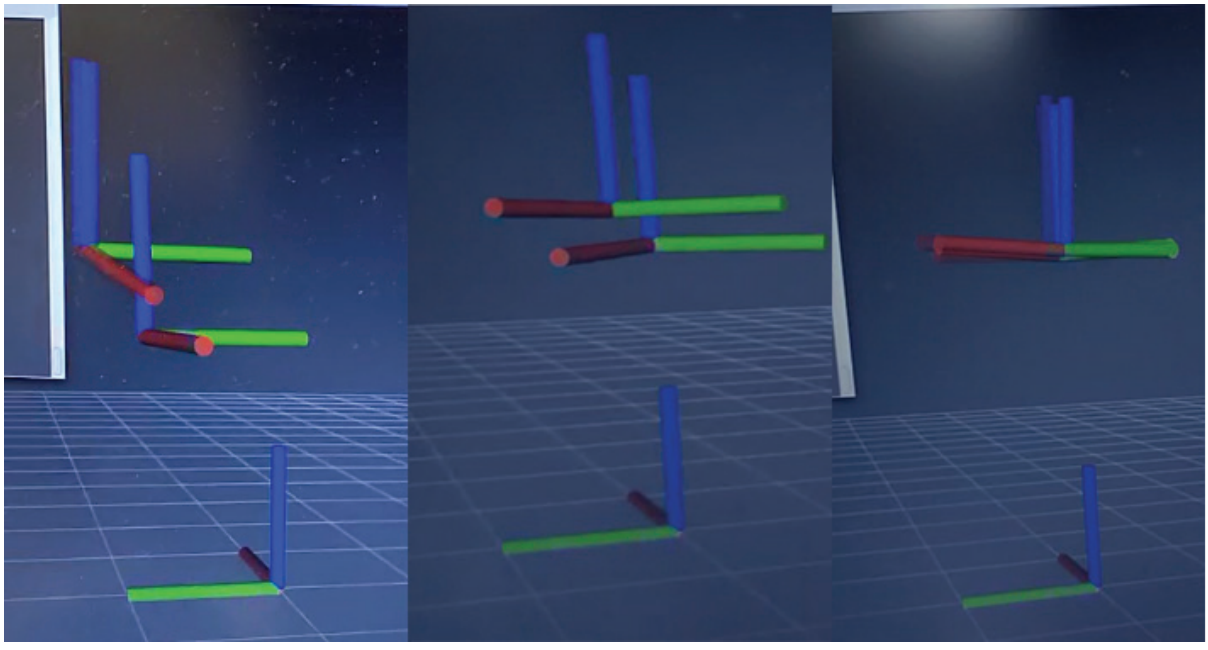

Fig. 12. Comparison of pose estimation without (extreme left) and with (extreme right) Kalman filter.

In Figure 12, the pose estimation is being shown, where the axes on the ground represent the origin axes and the other two represent the exact and predicted positions of the UAV. As seen on the extreme left image, it is evident that the error between the predicted and exact positions has a large margin.

Further with Kalman filter, the margin of error reduces and further on enhancement of Kalman filter variables, the error margin is reduced and the results are seen on the extreme right frame of Figure 12.

6. Conclusion and Future Works

In the proposed algorithm model, it is observed that this approach of mapping the environment based on instinctive motion of UAV, together with localising the affected areas in the environment, was successful. The A* algorithm results, in generating the shortest path of the proposed indoor environment, were acceptable. It was evident with the sensor data results on the radiation level >100 mrem on sensor data representing 10 mrem/day was pointing to the areas affected by radiation during the surveillance of the indoor environment.

As the outcomes obtained using simulations are acceptable, it is concluded that the considered phenomena in the algorithms can be well represented in the fundamental components approach. Future work is aimed at developing a simplified model that will be able to reproduce the same results that are measurable by a typical microprocessor-based hardware controller. This, in turn, will narrow down the prediction algorithms dedicated to avoiding any disaster or accident in an indoor environment having radioactive nuclear elements.

References

Aleotti J, Micconi G, Caselli S, Benassi G, Zambelli N, Calestani D, Zanichelli M, Bettelli M, Zappettini A (2015). Unmanned Aerial Vehicle Equipped with Spectroscopic CdZnTe Detector for Detection and Identification of Radiological and Nuclear Material. In: *2015 IEEE Nuclear Science Symposium and Medical Imaging Conference (NSS/MIC)*, pp. 1–5. San Diego, CA, USA.

Bhattacharyya, U. and Baum, C. (2018). Estimating the Location of a Nuclear Source in a Three-Dimensional Environment Using a Two-Stage Adaptive Algorithm. In: *2018 IEEE 8th Annual Computing*

and Communication Workshop and Conference (CCWC), pp. 8–14. Las Vegas, NV, USA.

Cai, C., Carter, B., Srivastava, M., Tsung, J., Vahedi-Faridi, J. and Wiley, C. (2016). Designing a Radiation Sensing UAV System. In: *2016 IEEE Systems and Information Engineering Design Symposium (SIEDS)*, pp. 165–169. Charlottesville, VA, USA.

Čerba, Š., Lüley, J., Vrban, B., Osuský, F. and Nečas, V. (2020). Unmanned Radiation-Monitoring System, *IEEE Transactions on Nuclear Science,* 67(4), pp. 636–643.

Duck, A., Munasinghe, K. S. and Reakes, T. (2017). Gas and Radiation Sensor Array for Deployment on UAV, ROV and as a Handheld Standalone Device. In: *2017 Eleventh International Conference on Sensing Technology (ICST),* pp. 1–5. Sydney, NSW, Australia.

Hartman, J., Barzilov, A. and Novikov, I. (2015). Remote Sensing of Neutron and Gamma Radiation using Aerial Unmanned Autonomous System. In: *2015 IEEE Nuclear Science Symposium and Medical Imaging Conference (NSS/MIC)*, pp. 1–4. San Diego, CA, USA.

Krátký, V., Petráček, P., Báča, T. and Saska, M. (2021). An Autonomous Unmanned Aerial Vehicle System for Fast Exploration of Large Complex Indoor Environments. *Journal of Field Robotics*, 38, pp. 1036–1058.

Micconi, G., Aleotti, J. and Caselli, S. (2016). Evaluation of a Haptic Interface for UAV Teleoperation in Detection of Radiation Sources, 2016. In: *18th Mediterranean Electrotechnical Conference (MELECON),* pp. 1–6. Lemesos, Cyprus.

Morita, T., Oyama, K., Mikoshi, T. and Nishizono, T. (2018). Decision Making Support of UAV Path Planning for Efficient Sensing in Radiation Dose Mapping. In: *2018 IEEE 42nd Annual Computer Software and Applications Conference (COMPSAC)*, pp. 333–338. Milwaukee, WI, USA.

Pani, R., Camera, F., Pergola, A., Polito, C., Falconi, R., Franciosini, G., Longo, M., Bettiol, M., Frantellizzi, V., de Vincentis, G., & Pani, A (2019). Novel Gamma Tracker for Rapid Radiation Direction Detection for UAV Drone Use. In: *2019 IEEE Nuclear Science Symposium and Medical Imaging Conference (NSS/MIC),* pp. 1–3. Manchester, UK.

Reyes Munoz, A., Pastor Llorens, E., Barrado Muxi, C. and Gasull, M. (2015). Monitoring Radiological Incidents through an Opportunistic Network. *IEEE Latin America Transactions,* 13(1), pp. 54–61.

Rudolph, C., Knoedler, B. and Heinskill, J. (2020). Comparable Data Evaluation Method for a Radio-Nuclear Sensor When Used on an UAV. In: *2020 IEEE SENSORS*, pp. 1–4. Rotterdam, Netherlands.

Seo, J.W., Han, S. H. and Young Shin, S. (2021). Deep Learning Based Nuclear Power Plant Monitoring System using UAV. In: *2021 International Conference on Electronics, Information, and Communication (ICEIC)*, pp. 1–4. Jeju, Korea (South).